



## MPPT OF SMALL WIND TURBINE DIRECT- DRIVES AXIAL FLUX PERMANENT MAGNET SYNCHRONOUS GENERATOR

Magdy Khaled , M Kamal Ahmed , Mahmoud Elwany and Mahfouz Shalaby

Electrical Power and Machines Department, Faculty of Eng., Al-Azhar University, Cairo, Egypt.

[eng\\_magdikhaled@hotmail.com](mailto:eng_magdikhaled@hotmail.com)

### ABSTRACT

This paper introduces a creative strategy of a low-speed, direct-drive axial flux permanent magnet generator (AFPMSG) for a wind turbine power generation control system that is created utilizing scientific and logical techniques, dynamic model of the axial-flux generator created utilizing Simulink/MATLAB. A maximum power point tracking (MPPT) -based FOC control approach is applied to obtain maximum power from the variable wind speed. The simulation results demonstrate the correct execution of the created dynamic model of the AFPMSG, control approach and wind power generator system.

**Keywords :** Axial-Flux PM synchronous machines, Dynamic-Model, MPPT0

### الملخص العربي

تتبع نقطة القدرة العظمى MPPT للمولد التزامنى ذى المجال المحورى والمدار مباشرة بتوربينات الرياح الصغيرة يقدم هذا البحث إستراتيجية إبداعية لنظام التحكم في توليد الطاقة الكهربائية باستخدام المولد التزامنى ذى المجال المحورى (AFPMSG) المدار بتوربينات الرياح الصغيرة عند السرعة المنخفضة. تم دراسة تتبع نقطة القدرة العظمى MPPT لهذا المولد باستخدام نموذج ديناميكي و الذي تم إنشاؤه باستخدام MATLAB/ Simulink. تم تطبيق نهج التحكم بتوجيه المجال FOC القائم على تتبع نقطة القدرة القصوى (MPPT) للحصول على أقصى طاقة من سرعة الرياح المتغيرة. توضح نتائج المحاكاة التنفيذ الصحيح للنموذج الديناميكي الذي تم إنشاؤه ل AFPMSG ونهج التحكم ونظام مولد طاقة الرياح. تم التحقق من خوارزميات التحكم المختارة و المطبقة في نظام التحكم للمحول من جانب المولد. كان نظام التحكم قادرًا على زيادة الطاقة المستخرجة من الرياح إلى الحد الأقصى كما ينعكس من معاملات القدرة التي تم الحصول عليها خلال سيناريوهات المحاكاة المختلفة.

**الكلمات الداله:** توليد الطاقة الكهربائية ، توربينات الرياح ، المولد التزامنى ذى المجال المحورى ، تتبع نقطة القدرة العظمى.

### 1-INTRODUCTION

Axial Flux Permanent Magnet (AFPM) synchronous machines have been developing in prevalence and have gotten an expanding measure of consideration in direct drive wind control application [1-3]. Relies upon the flux flow in the air gap, the electromechanical energy change machines are classified as Radial and Axial Flux Machines. The working rule worried about both the machines is similar however changes in its structure. The AFPMSG was designed with a single rotor, a double-sided airgap, and stators. The isotropic rotor is placed between teeth of the double-sided stators as shown in Fig. 1.

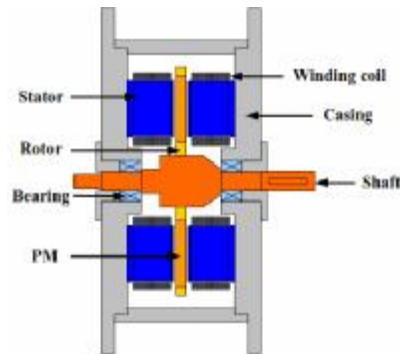


Figure 1: Cross section views of the AFPMSG

The stator back yokes are attached to the lateral case covers of the motor. The lateral case covers are made with rolled steel material. The stator teeth are individually fixed to the stator disk. The fan-shaped magnets of the rotor are mounted in holes of the rotor disk without the back yokes. Figure 2 shows the structure of the AFPMSG [1-4].

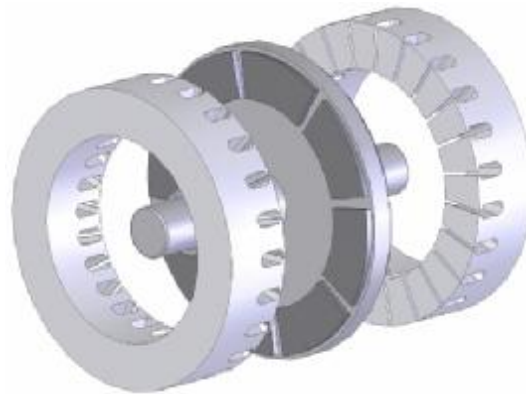


Figure 2: Magnetic circuit parts of an AFPMSG with a one rotor-two-stators.

Figure 2 shows that the magnets are installed on both sides of the disc rotor so that the flux of a pole travels through both magnets associated with the pole.

The main mechanisms of a direct-drive PM-synchronous generator are the wind turbine and the AFPMSG. The wind turbine captures the power from wind for the system, and the AFPMSG transforms the mechanical power into electric power. In this paper, the principles of the electric power generation will be introduced, and the mathematical-models of wind turbine and the AFPMSG will be developed and analyzed. These will further help in understanding the control procedures for the system as the following.

## 2- Dynamic Modeling of Wind Turbine

To explore the adequacy of the energy conversion in wind energy conversion systems, first the accessible energy put away in the wind should be resolved. The wind turbine demonstrate is known as the aerodynamic model concentrates control from the wind as motor vitality and afterward changes over it into mechanical vitality that is encouraged to the generator through a shaft. The aerodynamic power is given by to the following expression [7]:

$$P_m = \frac{1}{2} C_p(\lambda) \rho A U_w^3 \quad (1)$$

We shall use a generic equation of  $C_p$  as proposed by [8]. The equation is presented below as:

$$C_p(\lambda, \theta) = 0.22 \left( \frac{116}{\lambda_i} - 0.4\theta - 5 \right) e^{-\frac{12.5}{\lambda_i}} + 0.0068\lambda_i \tag{2}$$

And  $\frac{1}{\lambda_i} = \frac{1}{\lambda + 0.08\theta} - \frac{0.035}{1 + \theta^2}$  (3)

The affiliation between of Coefficient of power and Tip-speed ratio is given below.

The association between the tip-speed ratio  $\lambda$  and the rotor angular speed  $\omega_m$  (rads<sup>-1</sup>) is given as:

$$\omega_m = \frac{\lambda U_w}{R} \tag{4}$$

The association between the mechanical-torque  $T_m$  and the mechanical-power  $P_m$  is given by the equation below:

$$T_m = \frac{P_m}{\omega_m} \tag{5}$$

By substituting  $P_m$  from (1) and  $\omega_m$  from (4) into (5), the mechanical-torque  $T_m$  is given as:

$$T_m = \frac{1}{2} C_t \rho A R U_w^2 \tag{6}$$

Where  $C_t$  is the torque coefficient and is given below as:

$$C_t = \frac{C_p}{\lambda} \tag{7}$$

Figure 3 shows the relationship between the Coefficient of power (Cp) versus Tip-speed ratio (lambda). The Simulink-model of the wind turbine based on equations (1) to (7), is completed with the developed mechanical torque equation, is demonstrated in Fig. (4).

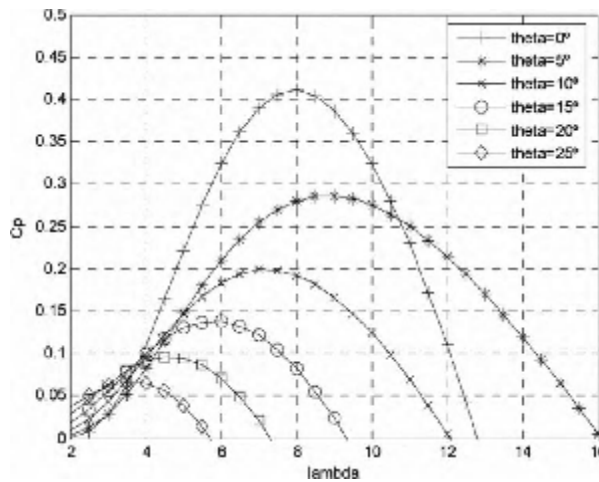


Figure 3: Coefficient of power (Cp) versus Tip-speed ratio (lambda)

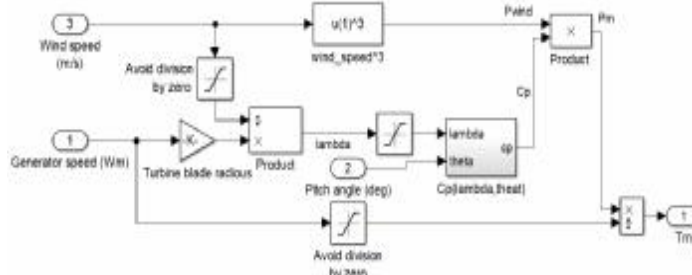


Figure 4: Wind turbine Simulink-model.

### 3- MATHEMATICAL MODELING OF PERMANENT MAGNET SYNCHRONOUS MACHINES

Permanent magnet synchronous machines /generators (PMSMs/AFPMSGs) play key role in direct-drive wind power-generation systems for transforming the mechanical power into electrical power. A rigorous mathematical modeling of AFPMSG is the prerequisite for the design of the machine control procedures as well as the examination of the steady-state and dynamic characteristics of wind energy conversion systems. The mathematical-model of a AFPMSG in both *abc* three-phase stationary reference frame and *d-q* synchronous-rotating reference frame will be developed, and the power and torque analysis of AFPMSGs will be given as well.

Before developing the mathematical-model of the AFPMSG, several important assumptions need to be made:

- (1) the damping-effect in the magnets and in the rotor, are insignificant;
- (2) the magnetic-saturation effects are ignored;
- (3) the eddy-current and hysteresis losses are ignored;
- (4) the back electromotive force (EMF) induced in the stator windings are sinusoidal;
- (5) for simplicity, all the equations of AFPMSMs are expressed in motor (consumer/load) notation, that is, negative current will be prevailing when the model refers to a generator.

Negative current means that at the positive polarity of the terminal of a device the current is out of that terminal. Figure 5 shows the Park transform for a three-phase AFPMSG generators. The stationary *abc* axes represent the path of the MMFs ( $f_a, f_b$  and  $f_c$ ) of the *a*, *b* and *c* phase-windings, which are induced by the time varying three-phase AC-currents in these stator-phase windings. The flux caused by the permanent magnet is in the direction of the *d*-axis fixed at the rotor. Here, the *d-q*-axes are revolving at the similar angular speed of the PMs and rotor. Also  $\theta_r$ , represents the angle between the *d*-axis and the stationary *a*-axis.

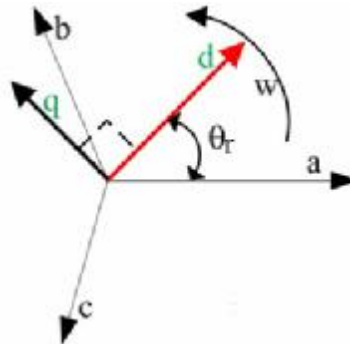


Figure 5: Park transform for AFPMSG generators.

The state space relationship of the terminal voltages of the AFPMSG to the phase currents and the phase flux linkages due to PMs and stator currents could be written as follows [9]:

$$\begin{bmatrix} v_{as} \\ v_{bs} \\ v_{cs} \end{bmatrix} = \begin{bmatrix} R_s & 0 & 0 \\ 0 & R_s & 0 \\ 0 & 0 & R_s \end{bmatrix} \cdot \begin{bmatrix} i_{as} \\ i_{bs} \\ i_{cs} \end{bmatrix} + \frac{d}{dt} \begin{bmatrix} \lambda_{as} \\ \lambda_{bs} \\ \lambda_{cs} \end{bmatrix} \quad (\wedge)$$

Where,  $v_{as}$ ,  $v_{bs}$ , and  $v_{cs}$  are the instantaneous *a*, *b*, and *c* three-phase stator voltages, and  $i_{as}$ ,  $i_{bs}$ , and  $i_{cs}$  are the instantaneous three-phase stator currents. Here,  $R_s$  is the stator-winding resistance per phase, and again,  $\lambda_{as}$ ,  $\lambda_{bs}$ , and  $\lambda_{cs}$  are the instantaneous flux linkages induced by the three-phase AC currents and PMs, which could be written in expanded form as follows [9]:

$$\begin{bmatrix} \lambda_{as} \\ \lambda_{bs} \\ \lambda_{cs} \end{bmatrix} = \begin{bmatrix} L_{aa} & L_{ab} & L_{ac} \\ L_{ba} & L_{bb} & L_{bc} \\ L_{ca} & L_{cb} & L_{cc} \end{bmatrix} \cdot \begin{bmatrix} i_{as} \\ i_{bs} \\ i_{cs} \end{bmatrix} + \begin{bmatrix} \lambda_r \cos(\theta_r) \\ \lambda_r \cos(\theta_r - \frac{2\pi}{3}) \\ \lambda_r \cos(\theta_r + \frac{2\pi}{3}) \end{bmatrix} \quad (9)$$

where,  $L_{aa}$ ,  $L_{bb}$ , and  $L_{cc}$ , are the self-inductances of the a, b, and c three-phases, and,  $L_{ab}$ ,  $L_{ac}$ ,  $L_{ba}$ ,  $L_{bc}$ ,  $L_{ca}$  and  $L_{cb}$  are the mutual-inductances between these phases, while,  $\lambda_r$ , is the rotor flux linkage caused by permanent magnet. The self-inductances and mutual inductances are all functions of  $\theta_r$ . Thus, all of the inductances are time varying parameters.

The  $dq0$ -Park's transformation is a mathematical transformation which aims to make simpler analysis of synchronous machinery models and was initial presented by R. H. Park in 1929 [10]. In three-phase systems like PMSMs, phase-quantities which include stator voltages, stator currents, and flux linkages, are time varying quantities. By applying Park's transformation, which is the projection of the phase quantities onto a rotating two axes reference frame, AC quantities are changed to DC quantities which are independent of time. The ( $abc$  to  $dq0$ ) transformation could be expressed in matrix form as follows:

$$\begin{bmatrix} v_d \\ v_q \\ v_0 \end{bmatrix} = \sqrt{\frac{2}{3}} \begin{bmatrix} \cos(\theta_r) & \cos(\theta_r - \frac{2\pi}{3}) & \cos(\theta_r + \frac{2\pi}{3}) \\ -\sin(\theta_r) & -\sin(\theta_r - \frac{2\pi}{3}) & -\sin(\theta_r + \frac{2\pi}{3}) \\ \frac{\sqrt{2}}{2} & \frac{\sqrt{2}}{2} & \frac{\sqrt{2}}{2} \end{bmatrix} \quad (10)$$

The inverse-Park's transformation is:

$$\begin{bmatrix} v_{as} \\ v_{bs} \\ v_{cs} \end{bmatrix} = \sqrt{\frac{2}{3}} \begin{bmatrix} \cos(\theta_r) & -\sin(\theta_r) & \frac{\sqrt{2}}{2} \\ \cos(\theta_r - \frac{2\pi}{3}) & -\sin(\theta_r - \frac{2\pi}{3}) & \frac{\sqrt{2}}{2} \\ \cos(\theta_r + \frac{2\pi}{3}) & -\sin(\theta_r + \frac{2\pi}{3}) & \frac{\sqrt{2}}{2} \end{bmatrix} \quad (11)$$

In expressions (10) and (11), and could represent stator voltages, stator currents or flux-linkages of AC machines, correspondingly. Considering that under balanced conditions,  $v_0 = 0$ , the voltage function of AFPMSG in  $d-q$  axes reference frame can be specified as follows [9]:

$$v_{ds} = R_s i_{ds} + L_d \frac{di_{ds}}{dt} - \omega_e L_q i_{qs} \quad (12)$$

$$v_{qs} = R_s i_{qs} + L_q \frac{di_{qs}}{dt} + \omega_e L_d i_{ds} + \omega_e \lambda_r \quad (13)$$

Where,  $v_{ds}$  and  $v_{qs}$ , are the instantaneous stator voltages in  $d-q$  axes reference frame, and  $i_{ds}$  and  $i_{qs}$ , are instantaneous stator currents in  $d-q$  axes reference frame. Here,  $L_d$  and  $L_q$ , are  $d$ -axis and  $q$ -axis inductances, and  $\omega_e$  is electrical angular speed of rotor, while,  $\lambda_r$ , is peak/maximum phase flux linkage due to the rotor-mounted PMs. Rendering to expressions (12) and (13), equivalent circuits of AFPMSG in  $d-q$  axes reference frame could be drawn as visible in Figure 6:

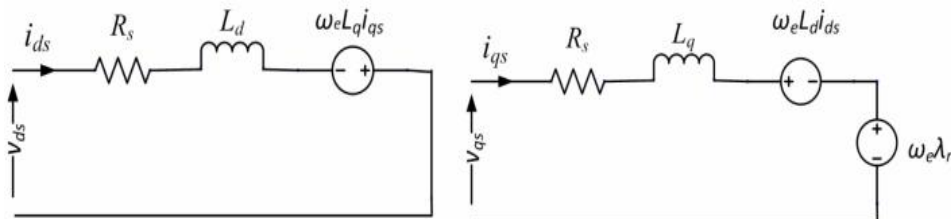


Figure 6: The  $d-q$  axes equivalent circuits of AFPMSG in (consumer/load) notation

According to assumptions, electrical power input could be definite in the *abc*- reference frame as follows:

$$P_{abc} = v_{as}i_{as} + v_{bs}i_{bs} + v_{cs}i_{cs} \tag{14}$$

or in the *d-q* axes reference frame as:

$$P_{dq} = \frac{3}{2} (v_{ds}i_{ds} + v_{qs}i_{qs}) \tag{15}$$

As a part of input-power, in motoring mode, the active power is the power that is transformed to mechanical-power by the machine, which can be stated as:

$$P_{em} = \frac{3}{2} (e_d i_{ds} + e_q i_{qs}) \tag{16}$$

where,

$$e_d = -\omega_e L_q i_{qs} - \omega_e \lambda_q \tag{17}$$

$$\text{and } e_q = \omega_e L_d i_{ds} + \omega_e \lambda_r = \omega_e \lambda_d \tag{18}$$

Here,  $e_d$  and  $e_q$ , are the back EMFs in the *d-q* axes reference frame, and  $\lambda_d$  and  $\lambda_q$  are the *d-q* axes flux linkages. Substituting expressions (17) and (18) into (16), the active power could be re-expressed as:

$$P_{em} = \frac{3}{2} \omega_e (\lambda_d i_{qs} - \lambda_q i_{ds}) \tag{19}$$

Hence, the electromagnetic torque developed by a AFPMSG can be deduced as:

$$T_e = \frac{P_{em}}{\omega_e / \frac{p}{2}} = \frac{3}{2} \left( \frac{p}{2} \right) (\lambda_d i_{qs} - \lambda_q i_{ds}) \tag{20}$$

$$\text{Or } T_e = \frac{3}{2} \left( \frac{p}{2} \right) (\lambda_r i_{qs} + (L_d - L_q) i_{qs} i_{ds}) \tag{21}$$

where,  $p$  is the number of poles in the machine.

Simulink-model of AFPMSG based on equations (10) to (21), is completed with developed electromagnetic torque equation, are showed in Fig. 7:

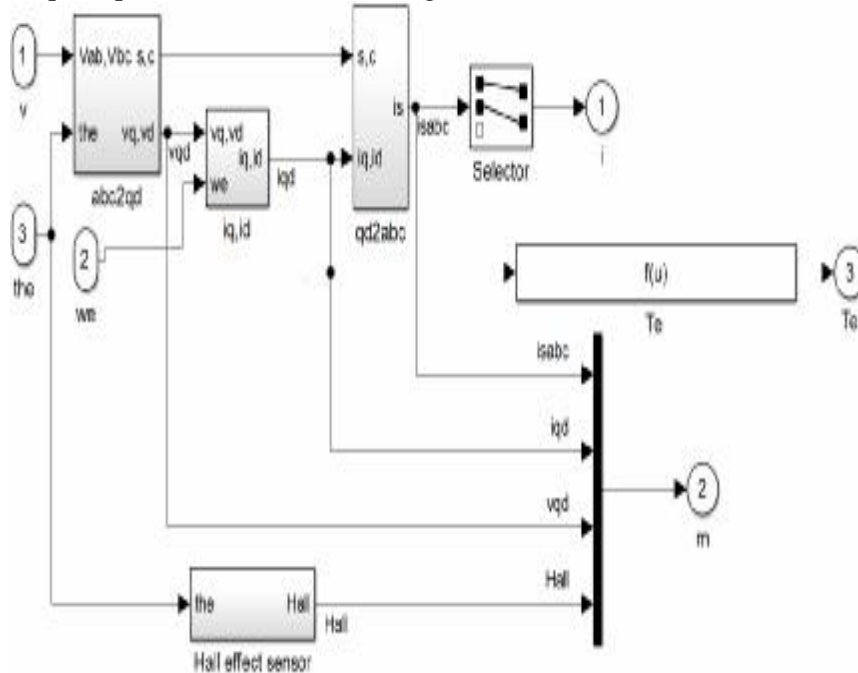


Figure 7: Dynamic-model of AFPMSG.

#### 4- CONTROL OF GENERATOR-SIDE CONVERTER

In wind turbine AFPMSG systems, three system variables need to be strictly controlled [11]:

- (1) the optimal power generated by the AFPMSG at different wind speed levels;
- (2) the active and reactive power injected into the grid;
- (3) the DC bus voltage of the back to back converter.

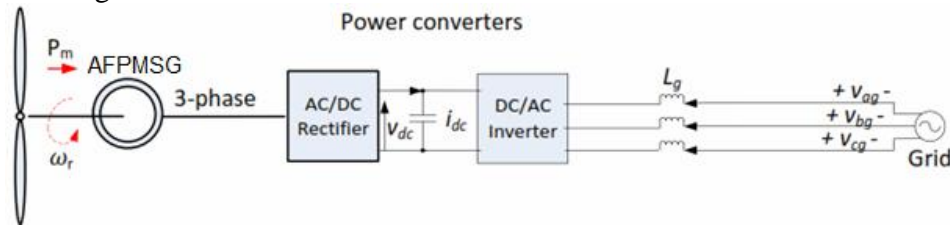


Figure 8: Direct-drive AFPMSG system

Figure 8 shows a direct-drive wind turbine AFPMSG fed by a back-to-back converter. In this system, the generator-side converter regulates the speed of the AFPMSG to implement the MPPT control. Meanwhile, the grid-connected converter controls active and reactive power injected into the grid.

#### 4-1 Maximum Power Point Tracking Control

Direct-drive AFPMSGs have the capability to work in a wide speed range. According to the intensity of the wind, the wind turbine generators need to be controlled to operate in three different modes as shown in Figure 9 [11]:

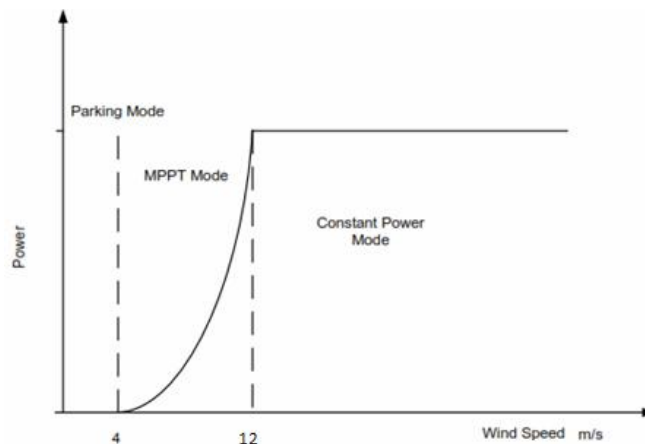


Figure 9: Wind turbine power-speed characteristic for the specific wind turbine

1. Parking Mode: when the wind speed is lower than the cut-in speed which is 4m/sec in this system, the wind turbine will not rotate but stay in parking status due to the fact that the electrical power generated by the AFPMSG system is insufficient to compensate for the internal power losses in this system. Therefore, the wind turbine is kept in parking mode by a mechanical brake;
2. MPPT mode: when the wind speed is greater than the cut-in speed, the wind turbine system starts to work and generate electrical power. Because the wind speed is in a relatively low range in the MPPT mode, the power captured by the wind turbine is below its rated value, the MPPT control needs to be applied to ensure a maximum efficiency of power capture. The MPPT mode ends when the wind speed is greater than the rated wind speed, 12 m/sec, for this case-study system.
3. Constant power region: when the wind speed becomes greater than the rated value, the power generated by the system will be larger than its rated power if the MPPT control is still applied. This will increase the electrical stress on the AFPMSG and the power processing devices, and would

further damage them. Therefore, the blade angle of the wind turbine blades needs to be properly controlled in the strong wind range to keep the system operating within its rated output condition. As its name implies, this is constant power region. As shown in equation (1), to control the captured mechanical power,  $P_m$ , at given wind speed,  $U_w$ , the only controllable term is the power coefficient,  $C_p(\lambda)$ .

The power coefficient characteristic is shown in Figure 3. As can be seen in this figure, different power coefficient curves correspond to different blade angles. For each case, there is an optimal tip speed ratio,  $\lambda$ , which contributes to a peak power coefficient value which, in turn, leads to a maximum power capture,  $P_m$ . In the MPPT operation mode, the pitch angle is usually kept at zero degree.

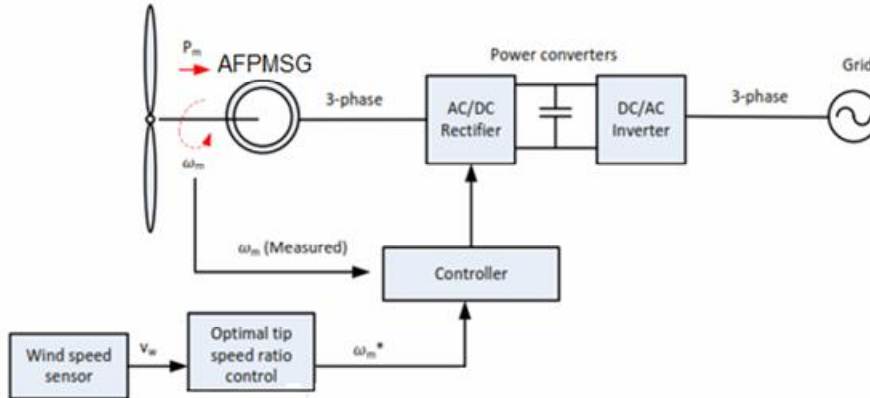


Figure 10: Tip speed ratio control scheme

In order to achieve the peak power coefficient value in the zero-degree pitch angle curve in Figure 3, the tip speed ratio needs to be controlled at the optimal value. From expression (1), the control of the tip speed ratio is actually the control of the rotor speed of the AFPMSG. A simplified scheme of tip speed ratio control is shown in Figure 10. From this figure, the wind speed information is sensed by a sensor and sent to a microcontroller, from which the reference speed of the AFPMSG can be calculated rendering to the optimum tip speed ratio.

Consequently, generator speed will reach its reference value in static-state, and then MPPT control is achieved.

#### 4-2 Field Oriented Control of the AFPMSG

The FOC approach was pioneered by F. Blaschke in 1970s [12]. The FOC approach has been and continues to be a significant factor in AFPMSGs control. In FOC approach,  $d$ - $q$  axes are rotating at rotor electrical angular speed with  $d$ -axis aligned with rotor flux path. Thus, flux creating current component,  $i_{ds}$ , and current component producing torque,  $i_{qs}$ , are along  $d$ -axis and  $q$ -axis, correspondingly. Thus,  $d$ - $q$  axes currents could be precise independently by two closed-loop controls in the FOC approach. The FOC approach, although its implementation requires large computational effort including PI control and coordinate transformations, it possesses the following merits: (1) fast speed and torque response; (2) outstanding low speed performance; and (3) low current and torque ripples. For the application of direct-drive AFPMSG systems, the AFPMSGs are directly driven by the wind turbine without a gearbox, which means that their operation speeds are always in a relatively low range. Moreover, the torque ripples of the direct-drive AFPMSGs should be controlled at a low level to decrease the mechanical stresses on the wind turbine. On the basis of the analysis above, the FOC approach was found to be more suitable for the direct-drive AFPMSG systems.

For a surface, mounted PM machine (SPM) which is applied in the case study system, the  $d$ -axis and  $q$ -axis inductances are equal. Thus, the torque expression equation (21) can be simplified and rewritten as follows:

$$T_e = \frac{3}{2} \left( \frac{P}{2} \right) \lambda_r i_{qs} \tag{22}$$

In order to reach maximum torque per ampere,  $d$ -axis current is set at zero.

Thus, there will be a linear affiliation among electromagnetic torque and  $q$ -axis current, such that the electromagnetic torque can be simply controlled by regulating of  $q$ -axis current.



The phasor diagram for FOC approach is exposed in Figure 11, and the control system of the generator-side converter is exposed in Figure 12.

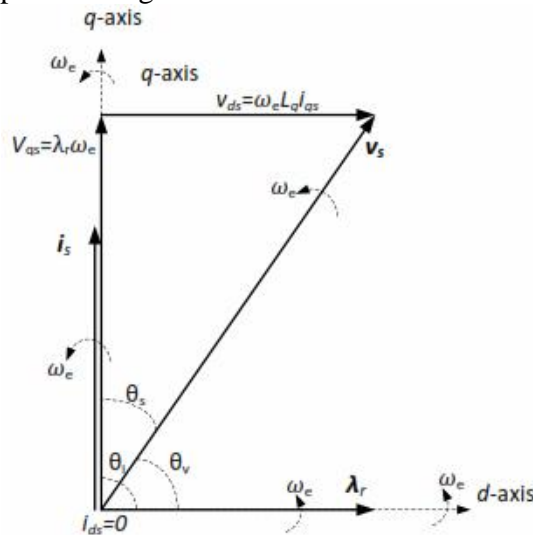


Figure 11: Phasor-diagram of FOC

As stated earlier, the FOC approach coupled to the optimum tip speed ratio based MPPT control strategy is applied here as the control algorithm for generator-side power converter. In Figure 12, there are three feedback loops in the control system which are: (1) the speed control loop, (2) the *d*-axis current control loop, and (3) the *q*-axis current control loop. In the speed loop, at every sampling time, the actual speed of generator sensed by an encoder mounted on the shaft of the rotor is compared to its reference value, which in turn is generated by the optimal tip speed ratio control, and then the error is sent to a PI controller which will output the reference *q*-axis current, meanwhile, the reference *d*-axis current, is always set to zero.

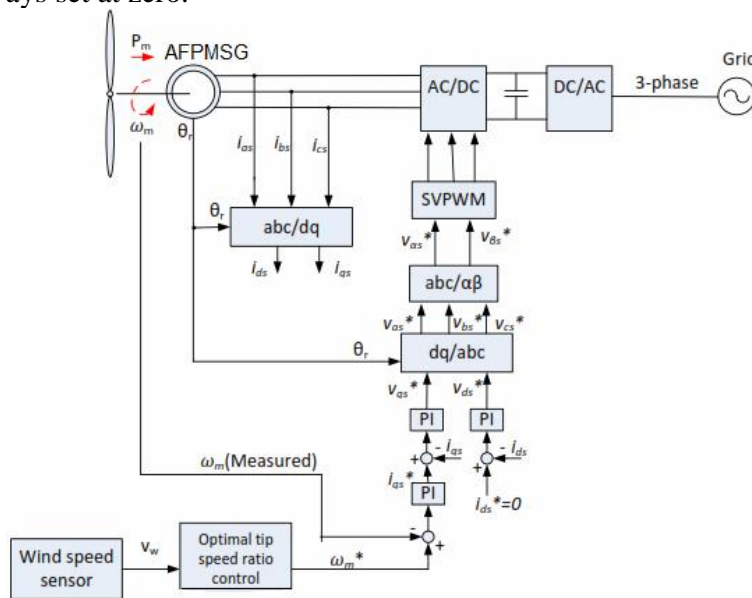
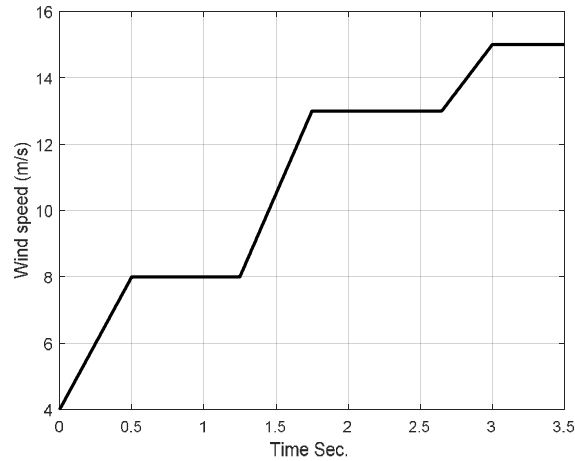


Figure 12 Generator-side control scheme

To obtain the response current signals, three-phase stator currents are sensed and transformed into *d-q* axes reference frame according to Park's-transformation. The reference stator voltages are then being accomplished by PI controllers in *d-q* axes current regulator loops. Here, space vector pulse width modulation (SVPWM) approach is applied as the modulation strategy in this system, because it generates less harmonic distortion in the output stator voltages/currents and provides more efficient



with the high wind speed can be investigated. Shown in Figure 15 is the actual rotor speed rpm. Figure 16 shows the corresponding three-phase stator currents. The  $d$ -axis and  $q$ -axis currents are shown in Figure 17 and Figure 18, respectively. Meanwhile, Figure 19 shows the electromagnetic torque developed by the generator. The electrical power developed by the generator is shown in Figure 20.



**Figure 14: Wind speed input**

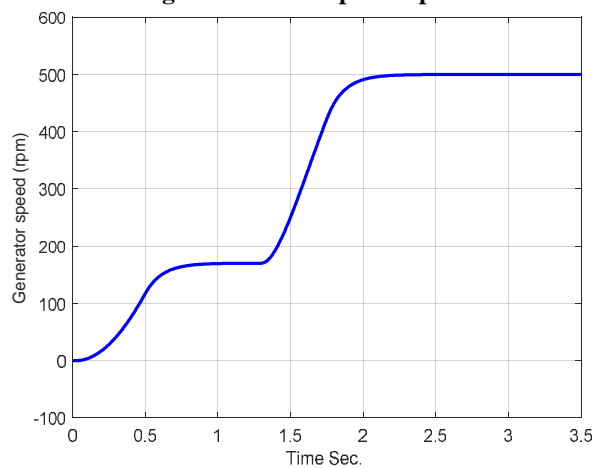


**Figure 15: Speed of the AFPMSG.**

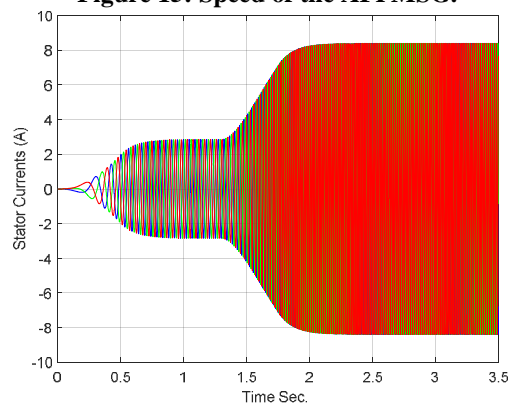


**Figure 16: Three-phase stator currents**

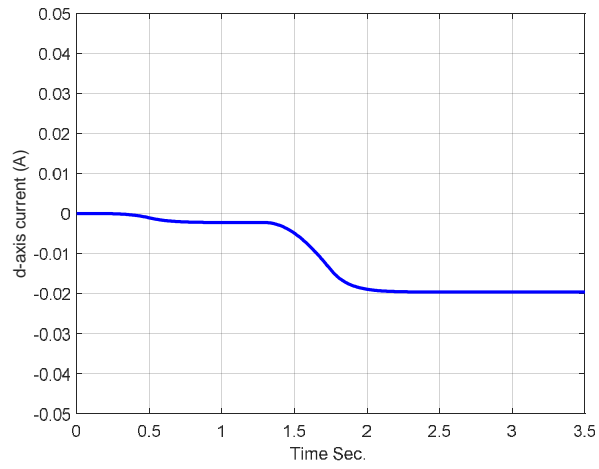


**Figure 17: d-axis current.**

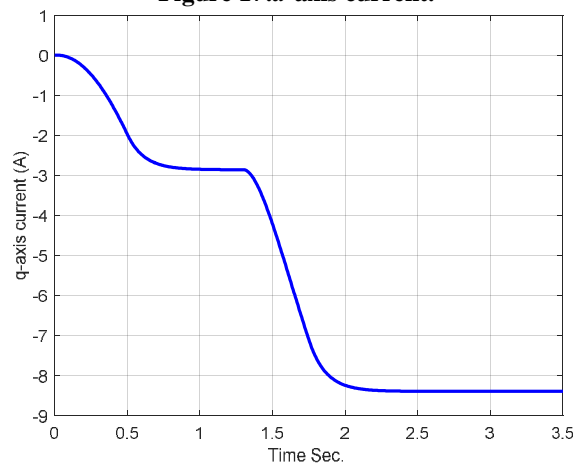


**Figure 18: q-axis current.**

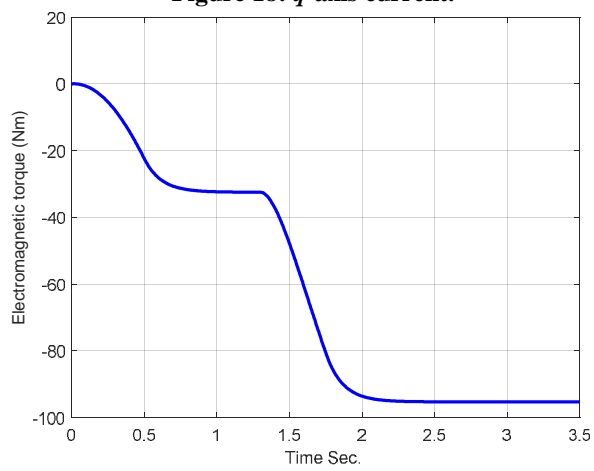


**Figure 19: Electromagnetic torque.**

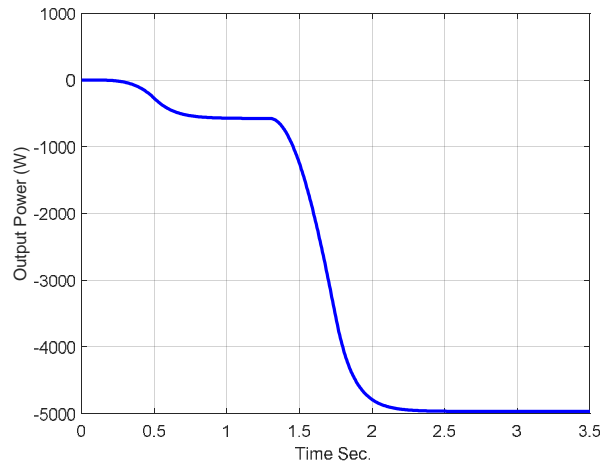


**Figure 20: Electrical power generated.**

As can be seen in the simulation results, according to different wind speed levels, the system performance has different characteristics best described as follows:

(1) From 0-1.3s: the wind speed starts to increase from the cut-in speed (4m/sec), which means that the generated electrical power is sufficient to compensate for the internal power consumption losses. Thus, the wind turbine begins to rotate and the AFPMSG begins to generate electrical power. As shown in Figures 15 through 20, with the increase of the wind speed, the stator currents, electromagnetic torque, and the generated electrical power are gradually increased. As can be seen in Figure 17, the  $d$ -axis current is controlled to be zero, which contributes to a linear relationship between the  $q$ -axis current and the electromagnetic torque. From 0.5s, the wind speed reaches and stops increasing, soon after that the system comes to the steady state. (2) From 1.3-2.6s: starting from 1.3s, the wind speed increases from 8m/s to 12m/s, which is the rated wind speed of the system. From 2.6-3.5s: the wind speed keeps increasing and exceeds the rated value. In order to limit the power input to prevent the electrical and mechanical stress on the system, the constant power control was applied in this wind speed range. That is, the mechanical power input of the system is kept at 5100w. and the generator speed is controlled at 4900 w instead of increasing with the wind speed.

## 6-CONCLUSION

The paper proposes a AFPMSG -based variable speed wind energy conversion system with a simple MPPT control strategy based on knowledge of wind turbine characteristics. Based on the simulation results and the analysis above, optimal power is generated by the AFPMSG wind turbine system at different wind speed levels. The chosen control algorithms applied in the control system of the generator-side converter are hence verified. The control system was able to maximize the energy extracted from the wind as reflected from the power coefficients obtained during the simulation scenarios considered.

## REFERENCES

1. Soderlund, L., Koski, A., Vihriala, H., Eriksson, J-T., Perala, R., Sep 1997, "Design of an Axial Flux Permanent Magnet Wind Power Generator", Eighth International Conference on Electrical Machines and Drives, (Conf. Publ. No. 444), vol., no., pp.224,228.
2. Chalmers, B.J., Wu, W., Spooner, E., "An Axial Flux Permanent Magnet Generator for a Gearless Jan 1996, "Wind Energy System", Proceedings of International Conference on Power Electronics, Drives and Energy Systems for Industrial Growth, vol.1, no., pp.610, 8-11.
3. S. Djebbari, J. F. Charpentier, F. Scuiller, and M. Benbouzid, 2016, "Design and Performance Analysis of Double Stator Axial Flux PM Generator for Rim Driven Marine Current Turbines," IEEE Journal of Oceanic Engineering, vol. 41, pp. 50-66.

4. M. Aydin, S. Husang, and T. A. Lipo, 2001, "Optimum design and 3D finite element analysis of non-slotted and slotted internal rotor type axial flux PM disc machines", *Power Engineering Society Summer Meeting*, pp. 1409-1416.
5. F. Caricchi, F. Crescimbeni, O. Honorati, and E. Santini, 1992 "Performance evaluation of an axial flux PM generator", *Proceedings of International Conference on Electrical Machines (ICEM)* , pp. 761-765.
6. R. J. Hill-Cottingham, P. C. Coles, J. F. Eastham, F. Profumo, A. Tenconi, G. Gianolio, 2001, "Multi-disc axial flux stratospheric propeller drive", *Proc. of IEEE IAS Annual Meeting Conference Record 2001*, vol. 3, pp. 1634-1639.
7. U. K. Mirza, N. Ahmad, T. Majeed, and K. Harijan., 2007, "Wind energy development in Pakistan", *Renewable and Sustainable Energy Reviews*, Vol. 11, No. 9: pp.2179- 2190.
8. Siegfried Heier. "Grid Integration of Wind Energy Conversion Systems", John Wiley & Sons Ltd, 1998, ISBN 0-471-97143-X, New York, USA.
9. E. Fitzgerald, J. C. Kingsley, and S. D. 1990, Umans, *Electric Machinery*. New York: McGraw-Hill.
10. R. M. Park, July 1929 , "Two-reaction theory of synchronous machines, pt. I: Generalized method of analysis," *AIEE Trans.*, vol. 48, pp. 716–730.
11. B. Wu, Y. Lang, N. Zargari, and S. Kouro, 2011, "Power Conversion and Control of WindEnergy Systems". Hoboken, NJ: Wiley.
12. Blaschke, Felix. (1972), "The principle of field orientation as applied to the new TRANSVECTOR closed loop control system for rotating field machines." *Siemens review*34, no.5: 217-220.